Gmail Khush Dhaliwal <dhaliwalkhush62@gmail.com>

Final draft of the thesis

Abhishek Chaudhuri <abhishek@iisermohali.ac.in> Sun, Jun 14, 2020 at 8:16 PM
To: Khush Dhaliwal <dhaliwalkhush62@gmail.com>

Dear Khushmeet,

Here is the letter of endorsement :

I hereby, agree to the declaration in the thesis "Stochastic simulations for cellular cargo transport: Role of Dynein catch-bond" (submitted by Ms. Khushmeet Kaur Dhaliwal (Reg. No. MS15105) for the partial fulfilment of BS-MS dual degree programme of the Institute), as the supervisor and having examined the thesis, find the work done by the candidate satisfactory and recommend that the report be accepted.

Best wishes,

Abhishek

Dr. Abhishek Chaudhuri, Ph.D.
Associate Professor
Department of Physical Sciences
Indian Institute of Science Education and Research, Mohali
Sector 81, Manauli PO, S.A.S. Nagar,
Mohali (Punjab) 140306, INDIA.
Office : 2F11, Academic Block
Mobile: +91-9872125912

[Quoted text hidden]

Gmail Khush Dhaliwal <dhaliwalkhush62@gmail.com>

Endorsement Certificate

Dipanjan Chakraborty <chakraborty@iisermohali.ac.in> Mon, Jun 15, 2020 at 2:35 PM
To: Khush Dhaliwal <dhaliwalkhush62@gmail.com>

Certificate of Examination

This is to certify that the dissertation titled **"Stochastic simulations for cellular cargo transport: Role of Dynein catch-bond"** submitted by Ms. Khushmeet Kaur Dhaliwal (Reg. No. MS15105) for the partial fulfilment of BS-MS dual degree programme of the Institute, has been examined by the thesis committee duly appointed by the Institute. The committee finds the work done by the candidate satisfactory and recommends that the report be accepted.

Signed
Dipanjan Chakraborty
15.06.2020

Dr. Dipanjan Chakraborty
Assistant Professor
Department of Physics
Indian Institute of Science Education and Research (IISER) Mohali.
Manauli-140306
Punjab
Web:http://www.iisermohali.ac.in/faculty/dps/chakraborty
http://14.139.227.202/Faculty/dipanjan/

On 15-Jun-2020, at 2:26 PM, Khush Dhaliwal <dhaliwalkhush62@gmail.com> wrote:

<Thesis_MS15105.pdf>

Gmail Khush Dhaliwal <dhaliwalkhush62@gmail.com>

Endorsement: MS Thesis submission

Rajeev Kapri <rkapri@iisermohali.ac.in> Mon, Jun 15, 2020 at 3:30 PM
To: Khush Dhaliwal <dhaliwalkhush62@gmail.com>

Dear Khushmeet,

Here is my letter of endorsement :

I, as a thesis committee member, agree to the declaration in the thesis "Stochastic simulations of cellular cargo transport: Role of Dynein catch-bond" (submitted by Ms. Khushmeet Kaur Dhaliwal (Reg. No. MS15105) for the partial fulfilment of BS-MS dual degree programme of the Institute). I find the work done by the candidate satisfactory and recommend that the report be accepted.

Best wishes,

Rajeev Kapri

> On 06/14/20 at 03:06pm, Khush Dhaliwal wrote:
> > Dear sir,
> >
> > Please find attached the final version of my thesis (MS15105). Kindly have
> > a look at it, and any feedback would be appreciated.
> >
> > For the submission of the same, I'd need an endorsement letter from your
> > side. Kindly send it to me so that I can submit my thesis.
> >
> > Thanking you
> >
> > Sincerely
> > Khushmeet Kaur Dhaliwal
> > MS15105
>
>
>
> --
> Rajeev Kapri, PhD
> Associate Professor (Physics)
> Indian Institute of Science Education and Research Mohali
> Sector 81, S A S Nagar, PO Manauli, Punjab 140 306 INDIA
> Mobile: +91 9779 624 331

--
Rajeev Kapri, PhD
Associate Professor (Physics)
Indian Institute of Science Education and Research Mohali
Sector 81, S A S Nagar, PO Manauli, Punjab 140 306 INDIA
Mobile: +91 9779 624 331

Stochastic simulations for cellular cargo transport: Role of Dynein catch-bond

Khushmeet Kaur Dhaliwal

A dissertation to be submitted for the partial fulfilment of BS-MS dual degree in Science

Indian Institute of Science Education and Research, Mohali
May, 2020

Certificate of Examination

This is to certify that the dissertation titled **"Stochastic simulations for cellular cargo transport: Role of Dynein catch-bond"** submitted by **Ms. Khushmeet Kaur Dhaliwal (Reg. No. MS15105)** for the partial fulfilment of BS-MS dual degree programme of the Institute, has been examined by the thesis committee duly appointed by the Institute. The committee finds the work done by the candidate satisfactory and recommends that the report be accepted.

Dr. Rajeev Kapri Dr. Dipanjan Chakraborty Dr. Abhishek Chaudhuri

(Supervisor)

Dated: June 14, 2020

Declaration

The work presented in this dissertation has been carried out by me under the guidance of Dr. Abhishek Chaudhuri at the Indian Institute of Science Education and Research, Mohali.

This work has not been submitted in part or in full for a degree, a diploma, or a fellowship to any other university or institute. Whenever contributions of others are involved, every effort is made to indicate this clearly, with due acknowledgement of collaborative research and discussions. This thesis is a bonafide record of original work done by me and all sources listed within have been detailed in the bibliography.

Khushmeet Kaur Dhaliwal
(Candidate)

Dated: June 14, 2020

In my capacity as the supervisor of the candidate's project work, I certify that the above statements by the candidate are true to the best of my knowledge.

Dr. Abhishek Chaudhuri
(Supervisor)

Acknowledgements

I'd like to take this opportunity to thank my supervisor Dr. Abhishek Chaudhuri for the able guidance, timely support and all the encouragement provided by him, without which I'd have been unable to finish this thesis. I'd also like to thank my thesis committee members, Dr. Rajeev Kapri and Dr. Dipanjan Chakraborty, for their valuable inputs and support.

I thank all the SCMP group members, especially Dr. Nisha Gupta and Subhashree, for helping and encouraging me, as and when needed.

I'd like to make a special mention for my dear friends, Nitheesh and Nimisha, who have been a constant support system for me throughout this journey. They helped me sail through all the ups and downs and made me believe in myself even in the toughest of times. They'd go out of their way to cheer me up when I'd feel low.

There are a lot of other people, who have had a positive impact on my life. I can't thank them enough for all the love, support and care that they gave me. All of these people have helped me grow a lot as an individual.

I believe that wherever I am today, is because of my mother. She inculcated a habit of hard work in me since a very young age and she'd be actively engaged in helping me with my studies. I dedicate everything I am today, to her. I wish she were here to see me become who I am today and she'd have been proud of me for all of this. Thank you for everything and I dedicate all of this to you, mumma.

And lastly, I'd like to thank my family for believing in me and encouraging me to pursue my dreams. My father, especially, has always made sure I had everything I ever needed. Without his constant support, I'd never have been able to achieve any of this. My brother, Avneet, has always pushed me to perform my best. I'd say I'm rather lucky to have three parents and I'd like to thank my step-mother for being there for me when the times were the hardest! I couldn't have made it without you all!

Khushmeet Kaur Dhaliwal

List of Figures

List of Tables

Notations

MT	Microtubule
N_+	No. of Kinesin motors
N_-	No. of Dynein motors
n_+	No. of attached Kinesin motors
n_-	No. of attached Dynein motors
π_+	Attachment rate for Kinesin motors
π_-	Attachment rate for Dynein motors
ϵ_+	Detachment rate for Kinesin motors
ϵ_-	Detachment rate for Dynein motors
$p(n_+, n_-)$	Probability of finding the system with n_+ attached Kinesin and n_- attached Dynein motors
t	Time at a given instant
Δt	Time step
F_{s+}	Kinesin stall force
F_{s-}	Dynein stall force
F_{d+}	Dissociation force for Kinesin motors
F_{d-}	Dissociation force for Dynein motors
F_c	Co-operative force
E_d	Deformation energy
α	Dynein catch-bond strength
F_0	Force scale for deformation energy
v_{0+}	Kinesin motor velocity
v_{0-}	Dynein motor velocity
v_{F+}	Forward Kinesin velocity
v_{F-}	Forward Dynein velocity
v_{B+}	Backward Kinesin velocity
v_{B-}	Backward Dynein velocity
v_c	Cargo velocity

l_{0+}	Kinesin motor rest length
l_{0-}	Dynein motor rest length
k_+	Spring constant for Kinesin motors
k_-	Spring constant for Dynein motors
P_{a+}	Probability of attachment of a Kinesin motor to the MT
P_{a-}	Probability of attachment of a Dynein motor to the MT
P_{d+}	Probability of detachment of a Kinesin motor from the MT
P_{d-}	Probability of detachment of a Dynein motor from the MT
d	Step length
ξ	Viscosity of the medium
σ	Size of the cargo
F_{tot}	Total force experienced by the cargo
D	Diffusion constant
K_B	Boltzmann constant
T	Temperature
ζ	Friction constant
η	Thermal noise
t_m	Maximum time allowed for the system to evolve
P_{step}	Probability of a motor to take a step
k_{step}	Rate of a motor to take a step
x	Position of the cargo
τ	Mean residence time
γ	Mean distance that the cargo walks in a particular state

Contents

Abstract

Intra-cellular cargo transport on microtubule filaments is predominantly carried out by molecular motors such as kinesins and dyneins. In this thesis, we explore the dynamical properties of cargo transport using Brownian dynamics simulations and specifically look at the effect of the unique detachment characteristics of dynein observed in experiments. Dynein motors show a catch-bond behavior in their detachment rates. We model this behavior and incorporate the same in our simulations. We first look at unidirectional cargo transport in the presence of dynein motors alone. The effective unbinding rate and effective velocity of cargo in the presence of collective motors show behavior similar to that of a single motor. Next, we look at the competition between two sets of motors in bidirectional transport of cargo. We show that in the presence of a dynein catch bond, the transport properties exhibit non-monotonic features, which helps us to understand a paradox in bidirectional transport.

Chapter 1

Motor Proteins: An Introduction

A cell is the basic building block of any living organism and is a very complex system in itself. It consists of several organelles; some of them are membrane-bound, while others lack a membrane. The complexity of cells and their organelles increase as we go from unicellular organisms to multi-cellular organisms or from prokaryotes to eukaryotes. Cells come together to form a tissue; several tissues join to form an organ, and so on. Each of their functions, down to the organelle-level, is highly specific and regulated. Such a complicated system requires regulated transport of materials from one part to another to maintain its stability. This task, within the cells, is carried out mostly by molecular motors, which are present inside the cytoplasm of the cell and move on the cytoskeletal tracks, either uni-directionally or bi-directionally, to transport cargo from one part to another [10, 24].

1.1 Cytoskeletal system

The cytoskeletal system of a cell is responsible for giving it shape and maintaining its structure. In a typical eukaryotic cell, the cytoskeletal system consists of actin filaments, microtubule filaments, and intermediate filaments, laid in the cytoplasm of the cell. Actin filaments (or microfilaments) are polymers of 'actin' proteins. Along with Myosin motors, these actin filaments generate contractile forces, leading to muscle contraction [3]. Intermediate filaments are mostly known to form cell-cell junctions, apart from providing structural stability to the cell [6].

Microtubule filaments are polymers of tubulin proteins, majorly known for carrying out intracellular transport in association with molecular motors. Three families of molecular motors are known to be associated with these filaments, which play a pivotal role in the transportation of cellular cargo [22].

1.2 Molecular Motors

Molecular motors are proteins, associated with the cytoskeletal system of the cell, that carry out mechanical work by deriving energy from ATP hydrolysis [9]. These motors are mostly responsible for intracellular transport of sub-cellular cargo like mRNA particles, organelles, virus particles, etc. and require a polar track for their movement [25]. Three families of molecular motors are known: kinesins, dyneins, and myosins. Myosins move on actin, whereas kinesin and dynein move on microtubule filaments to transport cargo. There are no known non-polar molecular machines that move on intermediate filaments. These motor families are known to travel predominantly in one direction, either plus-end (mostly towards the cell periphery) or minus-end (mostly towards the nucleus), depending on the polarity of the structural network [10]. The information on the polarity of actin and microtubule filaments is provided by the uniform molecular orientation of their subunit proteins. These motors move by generating a force large enough to transport cargo through viscous cytoplasm. Each of these motor proteins has two motor domains, which need to be highly coordinated in order to have a regulated transport of cargo. The importance of cargo transport by molecular motors can be understood by the fact that mutations in these molecular motors lead to several diseases [21].

1.2.1 Myosin motors

Myosins are a family of molecular motors which are known to take part in cellular transportation with the help of actin filaments [3].

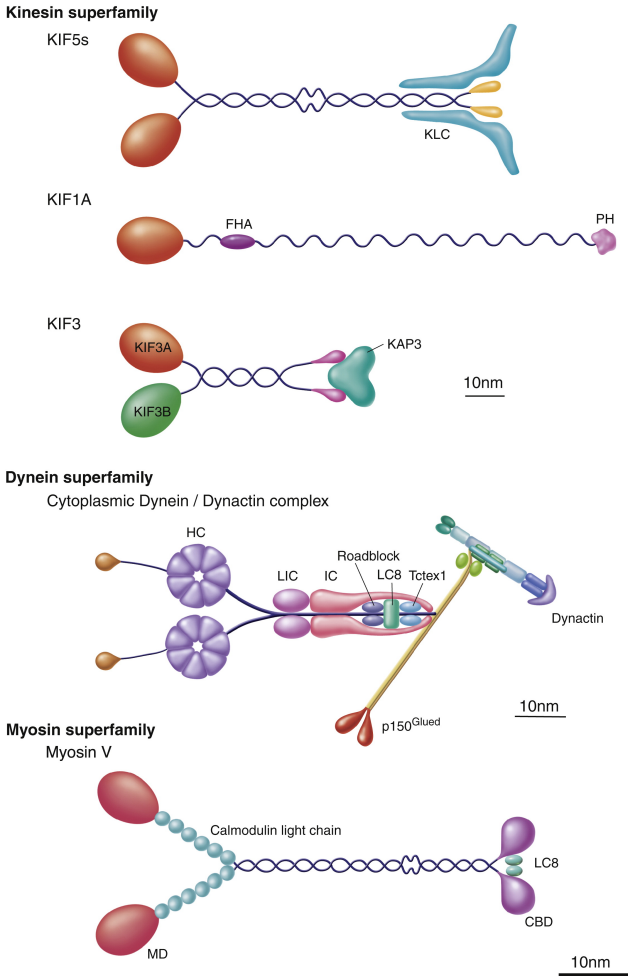

Figure 1.1: Structure of different families of motor proteins. Taken from [7].

1.2.2 Kinesin motors

Kinesins are a family of molecular motors that mostly take part in plus-end directed transport of intracellular cargo by moving along the microtubule filaments. Kinesin motor proteins form tetramers, with two Kinesin heavy chains (KHC) and two Kinesin light chains (KLC), forming two 'motor' domains, a stalk, and a 'tail' domain [8]. The tail domain is mostly distinct in different types of Kinesin motors suggesting their functional diversity. Tails attach to the cargo with the help of a receptor, while the motor domains move on the cytoskeletal filament [24]. These motors carry out mechanical work with a thermodynamic efficiency of ~40-60% [9].

1.2.3 Dynein motors

Cytoplasmic Dyneins are the only family out of the three families of molecular motors that take part in minus-end directed motion along the microtubules. Dynein motor proteins are formed of two heavy polypeptide chains, two intermediate polypeptide chains, four intermediate light chains, and several light polypeptide chains. The heavy chains form the 'head-like' structure for movement along the microtubules [7, 11]. There is another protein complex Dynactin which binds with Dynein motors and regulates its activity [7, 23]. Apart from the transport of cellular cargoes, Dyneins also play a crucial role in cell division [10].

Dynein shows an extremely interesting behavior in its detachment characteristics. Detachment rates of molecular motors from their filament tracks are measured using bead assay experiments [14]. In these experiments, cytoskeletal filaments are extracted in-vitro and are attached to a substrate. The bead held by optical tweezers is brought close to the surface-bound cytoskeletal filaments. Molecular motors attach to the filament, and load forces are applied via the bead on the molecular motors in a direction opposite to their direction of movement on the filament track. At a particular load force, the motor stalls. If forces are applied above the stall force, then the motor protein detaches from the filament. Thus the detachment rates are measured. For kinesins, the detachment rate increases as the external load force is increased: a characteristic feature of most bonds. This is called the *slip bond*. On the other hand, for dyneins, the detachment rate initially increases and then beyond a critical force, the detachment rate starts decreasing. This is a characteristic of a *catch bond*. When large forces are applied, dynein again starts showing the slip bond characteristics. This slip-catch-slip behavior of the detachment rate is important to consider when we look at transport properties of molecular motors [17].

Although the microscopic understanding of why such a behavior is seen in dyneins is not clear, it has been speculated that there is some sort of allosteric rearrangements that happen which leads to a lock-key system. The attachment of the dynein to the microtubule is a receptor (R) - ligand (L) binding. Upon increasing the load force, there is an allosteric deformation, which results in a locking of the receptor-ligand complex [15]. This prevents detachment of the

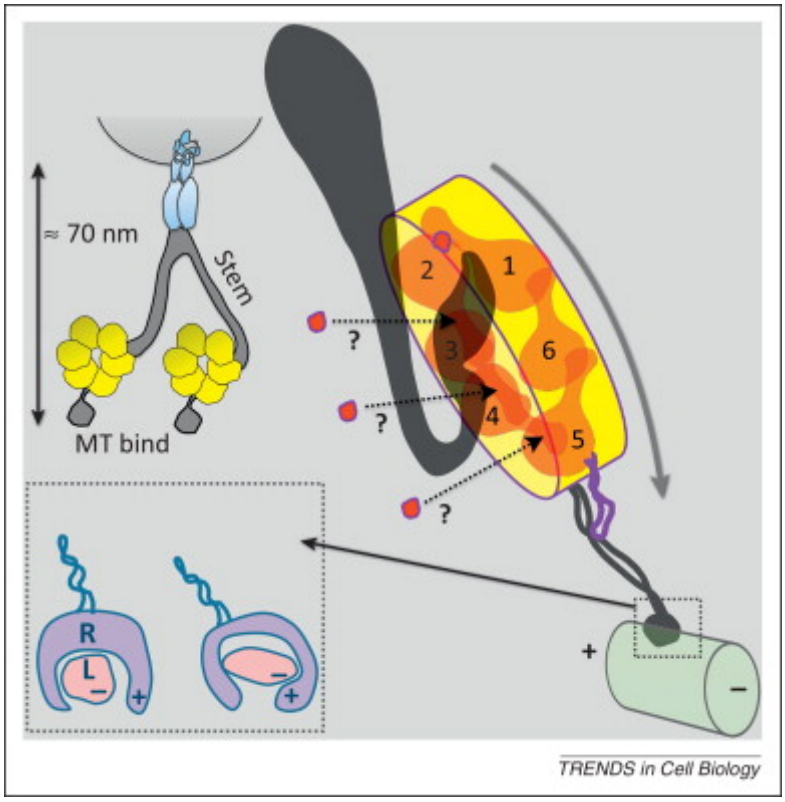

Figure 1.2: Dynein structure with the bead assay arrangement. The left inset shows the receptor-ligand lock-key mechanism. Taken from [15].

motor protein giving rise to the catch bond regime.

1.3 Plan of the thesis

In this thesis, I have explored the effects of incorporating catch-bond in dynein on transport properties of cargo in cells. Chapter 2 of the thesis will detail the Brownian dynamics simulation technique that I have used to explore the transport properties. Chapter 3 will talk about the results of the simulations for a cargo carried by only dynein motors. In Chapter 4, I will extend the simulations to that of a cargo carried by two sets of motors- kinesins and dyneins, and show that incorporating the catch bond behavior of dynein helps to explain some of the peculiar characteristics of cargo transport in cells. In Chapter 5, I will outline the mean-field theory, which is used to study bidirectional transport analytically.

Chapter 2

Model for cargo transport

As I have already mentioned, directional cargo transport in the cell happens with the help of molecular motors. I focus on transport of cargo on microtubule (MT). I will discuss Brownian dynamics simulations to model the transport of cargo via multiple molecular motors. The simulations are in one dimension which means that all the displacements, velocities and forces are directed along the MT. Molecular motors which attach and detach from the MT do not interact with one another. However, because of the forces that they apply on the cargo bead on attachment, they can affect one another via the bead.

2.1 Unidirectional transport

In unidirectional transport, the cargo is carried by one set of molecular motors - either kinesin motors or dynein motors. Since in this thesis we focus on the effect of dynein, we look at unidirectional transport of cargo due to dynein motors only. The details of the simulations are given below.

We consider a cargo being carried by N dynein motors. Now, each of the molecular motors can exhibit two states in such a system, either an 'attached' or a 'detached' state. As the names suggest, the attached state implies that the molecular motor is attached to the microtubule and the detached state implies that the molecular motor is detached from the microtubule filament. A detached motor can re-attach with a probability which is given by the attachment rate. Where it

attaches, depends upon the region which can be explored by the molecular motor. A motor which is attached can have 3 choices : (i) remain where it is (ii) move on the MT (iii) detach from the MT. In this situation how do we find out what the motor is supposed to do? We calculate the forces that the motor experiences, which depend upon the distance between the point where the motor is attached to the MT, and the point where it is attached to the bead. Once this is known, we update the position and state of the attached motor.

In a time step, once we have found the position and state of all the N motors, we update them simultaneously and find out the resultant position of the bead depending on the force it experiences. When there is no load force acting on the cargo bead, the molecular motors which are all of one type (dynein in our case) move the cargo bead in one direction. We apply a load force F in the direction opposite to the motion of the molecular motors. The molecular motors are modelled as elastic springs. The rest length of the spring is l_0 and the spring constant is k. Once the molecular motors are stretched beyond their natural length, only then they start generating restoring force. The algorithm for the update process is the following :

1. Initial condition : The simulations are started at $t = 0$ by keeping all the N motors in the attached state and by keeping the cargo bead at the origin. All the motors are clustered and attached to the bead at the same point. Each motor is permanently attached to the cargo on one side and to the microtubule filament within its rest length (in either direction) on the other side. Once the motor positions on the MT are fixed, we calculate the forces on the cargo bead due to the motors and the load force and determine the initial position of the bead.

2. A small time step is defined and at every time step, the state of the molecular motors and cargo is updated till a maximum time t_m. At a given time, this is what is done :

   (a) For $t > t_m$, go to (3).

   (b) Go to a motor and check if it is in the attached state or in the detached state.

(c) If detached, it is checked whether the motor will get attached to the MT or remain detached. The probability for the attachment of the motor is given by $P_a = \pi\Delta t$, where π is the attachment rate of the molecular motor. If the motor gets attached to the MT, it is positioned within its rest length on either side of the cargo and its state and position are updated.

(d) If attached, we first check the load force on the motor, which is calculated as the usual spring force $F_l = k\Delta l$. Here, Δl is the extension experienced by the motor beyond the rest length. We, then, check if the motor will get detached from the MT with a probability $P_d = \epsilon\Delta t$, where ϵ is the detachment rate. We will discuss the form of the detachment rate for dynein motors later. The detachment probability of the molecular motors, as mentioned earlier, depends on the load force experienced by them. If the motor gets detached, the state of the motor is updated.

(e) However, if the motor doesn't get detached from the MT, we check if the motor would take a step. The probability of taking a step is given as $P_{step} = k_{step}\Delta t$. The discussion for k_{step} is given later. If the motor takes a step, its position is updated from x_i to $x_i + d$ where d is the step length of the motor. This is in accordance with experiments on molecular motors.

(f) Update the position and states of all the N motors in one step.

(g) Update the cargo bead position as follows : As the extension in the molecular motors go beyond their rest length, restoring force comes into the picture and exerts a force on the cargo. Towards the end of each time step, the force exerted on the cargo by each of the motors is calculated and the total force on the cargo is given by $F_{tot} = \Sigma F_i$. The cargo not only experiences the restoring forces from the motors attached to it, but also the viscous and thermal forces. The viscosity of the medium is taken to be ξ and the diffusion constant is given as $D = k_B T/\zeta$ where the friction constant ζ is defined as $\zeta = 6\pi\xi\sigma$. Here, σ is the size of the cargo bead. The velocity with which the

cargo moves is given as $v_c = \frac{F_{tot}}{\zeta}$. Considering thermal noise (η) in the Langevin equation for an over-damped system, the position of the cargo is given as:

$$x\left(t+\Delta t\right) = x\left(t\right) + v_c \Delta t + \eta \tag{2.1}$$

The statistical properties of the noise is such that $\langle \eta\left(t\right)\rangle = 0$ and $\langle \eta\left(t\right)\eta\left(t'\right)\rangle = 2D\delta\left(t-t'\right)$.

3. Find the total distance travelled by the cargo.

Choosing k_{step}

In order to find out k_{step}, we first have to choose a force-velocity relation for molecular motors. A good approximation is one which assumes a linear decrease in the velocity of a motor with the force that is applied against its movement. Therefore,

$$v(F) = v_0\left(1 - \frac{F_i}{F_s}\right) \tag{2.2}$$

where v_0 is the unloaded velocity and F_s is the stall force of the motor, the force which brings the motor to a halt. Since the motor makes a step d, therefore, $k_{step} = v(F)/d$, for backward loads $F_i < F_s$. For $F_i > F_s$, $P_{step} = 0$. On the other hand, in presence of forward loads, we have $F_i = 0$.

Model for the detachment rate of dynein

As we mentioned in the introduction, there are two kinds of possible scenarios when we think of the detachment of molecular motors from the filament. The probability of the detachment can increase exponentially with increasing load : this is called the slip bond. We can model this bond by the following expression : $\epsilon = \epsilon_0 \exp(F/F_d)$ where ϵ_0 is the unloaded detachment rate and F_d is the detachment force which sets a scale. This expression is obtained from the idea of barrier crossing.

However dynein detachment characteristics suggests that it behaves as a catch-bond. In this case, the detachment rate decreases with increasing force. How

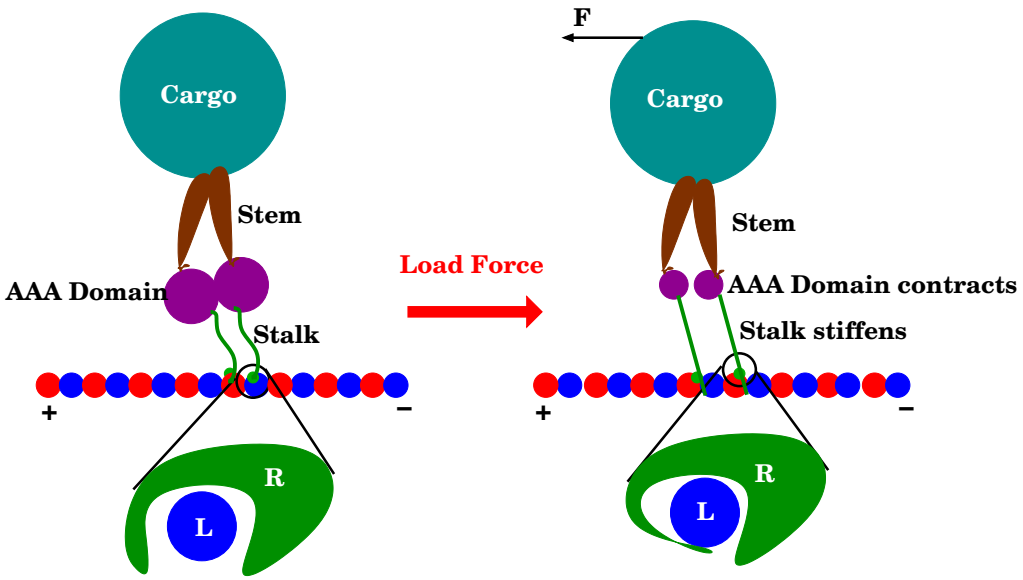

Figure 2.1: Schematic of conformation change in receptor-ligand binding giving rise to catch bond in dynein. Taken from [17].

can such behavior be modelled? There are several models which can capture this behavior [1, 2, 4, 18, 19]. Here I discuss three of them :

- Two pathway model : In this model, two paths are considered. One is the catch path which acts against the load force and another is the slip path which acts in favor to the load force. Therefore, there are two exponential forms one increasing with load and another decreasing with load. The detachment rate is then written as

$$\epsilon(F) = \epsilon_0^1 \exp\left(\frac{F}{F_d^1}\right) + \epsilon_0^2 \exp\left(-\frac{F}{F_d^2}\right) \tag{2.3}$$

  where $\epsilon_0^1, \epsilon_0^2$ are bare dissociation rates while F_d^1, F_d^2 set the force scales. We can get a catch-slip transition by tuning $\epsilon_0^1, \epsilon_0^2$.

- Bond deformation model : In this model, it is assumed that there is a bond deformation energy given as

$$E_d(F) = \alpha[1 - \exp(-\frac{F}{F_0})], \tag{2.4}$$

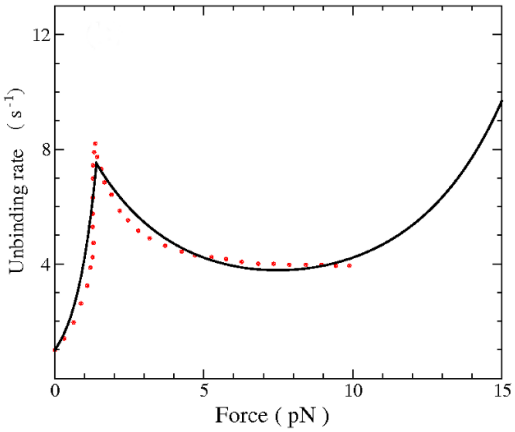

Figure 2.2: Dynein unbinding rate from experiments [13] (points) and fitting (solid line) to the TFBD model [17].

where α is strength of the deformation energy and F_0 is a force scale. This can be tuned in such as way that we can go from a slip to a catch like situation. The deformation rate is given as $\epsilon(F) = \epsilon_0^s \exp(-E_d(F)/k_BT)$.

- Threshold bond deformation model (TFBD) : In this model, it is realized that the dynein motor first shows a increase in detachment rate for small forces. Then after a critical force of $\sim$ 2pN, the rate starts decreasing which is catch bond. Then at large forces again the detachment rate increases. All of this can be taken into the bond deformation model picture by assuming that the deformation energy is of the following form :

$$E_d(F) = \Theta(F - F_s)\alpha \left[1 - \exp\left(-\frac{F - F_s}{F_0}\right)\right], \tag{2.5}$$

The unbinding rate is then given as

$$\epsilon(F) = \epsilon_0 \exp\left(-\frac{E_d(F)}{k_BT} + \frac{F}{F_d}\right) \tag{2.6}$$

where $\exp(\frac{F}{F_d})$ is the usual slip part. This model captures the slip-catch-slip behavior of dynein very well (see Fig. 2.2). We use this model in our simulations.

2.2 Bidirectional transport

To model the transport of a cargo under the influence of both kinesin and dynein motors on a MT track, we have two sets of motors attached to the cargo bead in our simulations. The parameters are given as ±, with + denoting kinesin parameters and − denoting dynein parameters. The set of parameters used in the simulation are given below. Note that the Brownian dynamics simulations proceed in exactly the same way as before. Starting with N_+ kinesin and N_- dynein motors, we run the simulations and the states and positions of all the motor proteins (both kinesin and dynein) are updated at the same time. Then the cargo position is updated according to the forces. Note that in this system since the two sets of motor proteins move in opposite direction on the MT track, there is always a load force acting on one set of motor proteins due to another even in the absence of an external load force. Further, the spring rest lengths of the kinesin and dynein are chosen differently. For kinesin, l_0 = 100nm and for dynein, l_0 = 50nm. The spring constant of both motors is k = 0.32pN/nm.

Parameters	**Kinesins**	**Dyneins**
$F_{s\pm}$	$6pN$	$1pN$ (Weak) $7pN$ (Strong)
$F_{d\pm}$	$3pN$	0.67 pN
$\pi_{0\pm}$	$5/sec$	$1/sec$
$\epsilon_{0\pm}$	$1/sec$	$(0.1-10)/sec$
$v_{F\pm}$	$0.65\mu m/sec$	$0.65\mu m/sec$
$v_{B\pm}$	$1nm/sec$	$1nm/sec$

Table 2.1: Parameter values for single-motor dynamics used in simulations. Taken from [20].

Chapter 3

Unidirectional Transport

In this chapter we present the results of simulations carried out for unidirectional transport. As we have mentioned, during unidirectional transport, only dynein motors attach to the cargo. Therefore, we switch off the kinesin motor part of the simulation. Since the dynein motors pull the cargo predominantly in one direction, left to itself, the cargo will show a uniform processivity in one direction. To see the effect of load force on the collective dynamics of the dynein motors, a force is applied to the cargo in the direction opposite to the direction of movement of the dynein motors. We study the transport properties of the cargo as a function of the force applied. The simulations are allowed to run for a long time till the cargo detaches from the filament. We average the results over 1000 initial conditions.

3.1 Results for a single dynein motor

In Fig. 3.1, we look at how the average unbinding rate of a cargo in the presence of a single dynein motor changes as the load force on the system is varied. We observe that the results obtained are exactly as expected. We see that initially the unbinding rate increases as the load force is increased. The rate increases till a critical value is reached. Beyond this point, we observe that the unbinding rate starts decreasing with increasing force, till a very large force is applied. Then the unbinding rate again starts to increase in an exponential manner. This plot indicates that dynein motors exhibit catch-bond behavior in a certain force range,

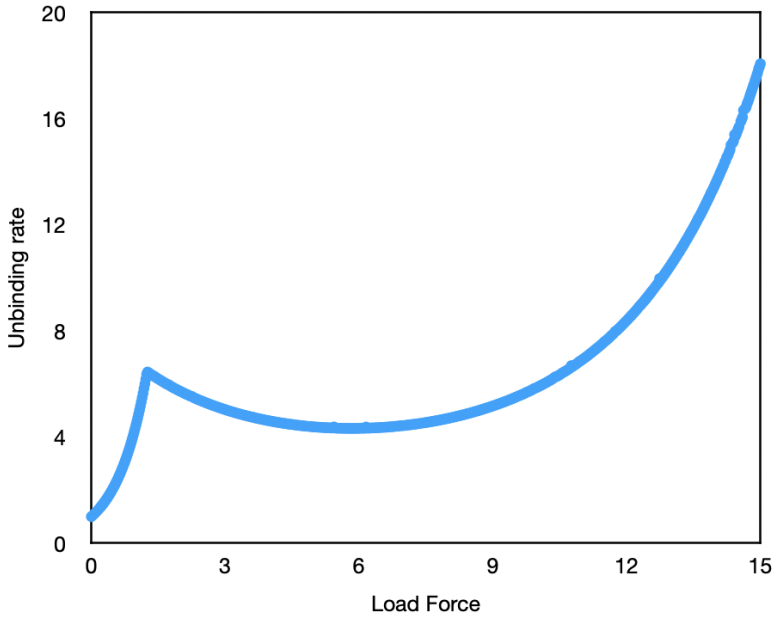

Figure 3.1: Simulation results showing dynein motor average unbinding rate as a function of load force.

thereby depicting slip-catch-slip kind of behaviour.

3.2 Results for multiple dynein motors

We look at the variation in average number of attached motors as the load force on the system is changed, in Fig. 3.2. Here, we have a system with five dynein motors. We see that the number of attached motors on an average decreases initially till the load force becomes equal to the stall force. The results obtained in Fig. 3.1 support this observation. As the unbinding rate increases with increasing force, it is expected that more and more motors would get detached from the MT filament in this regime, just as we observed. As the load force is increased beyond the critical value where the catch-bond steps in, the average number of motors attached to the microtubule increases depending on the value of the binding rate. The higher the binding rate, the more the number of motors get attached to the filament. This is the regime where catch-bond is active and lower number of motors detach from the filament in this regime. As the load force is increased further, motors

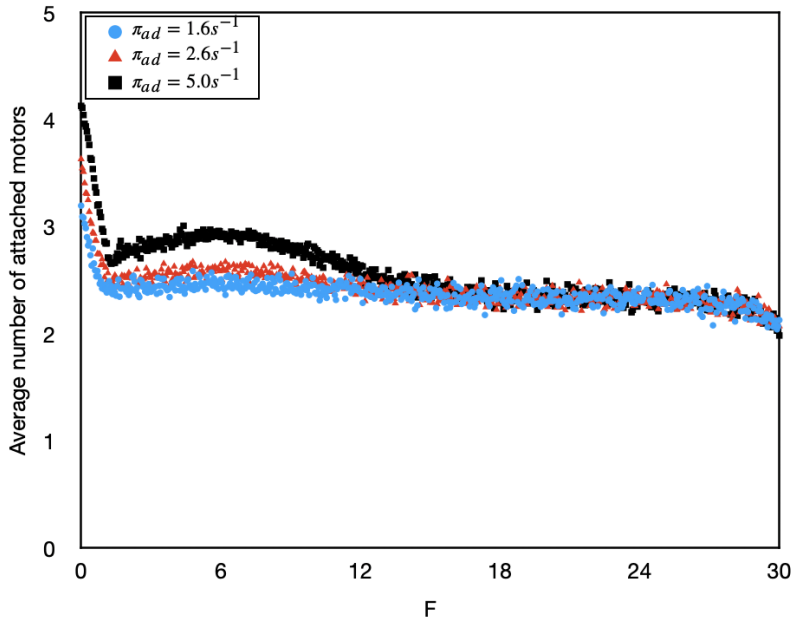

Figure 3.2: Average number of attached dynein motors (for a system with 5 dynein motors) as a function of load force for different rates of attachment of the motors.

start detaching from the filament as the unbinding rate again starts to increase with increasing force. Hence, these results also suggest that dynein motors bind to the microtubule in a slip-catch-slip type of behaviour, depending on the force experienced by the motor.

Fig. 3.3 shows the results of average cargo velocity as a function of load force. As expected from the model, we observe an almost linear decrease in the cargo velocity as the load force on the system increases.

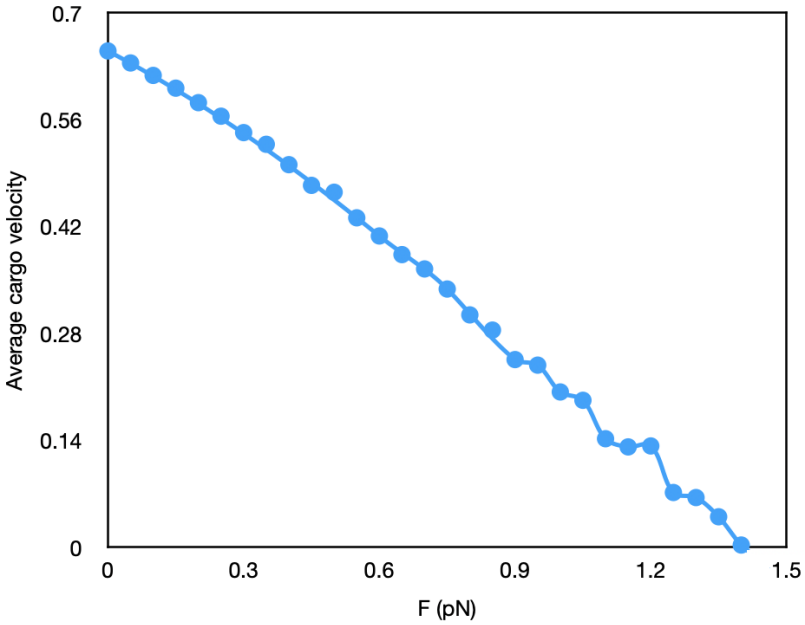

Figure 3.3: Average cargo velocity (in $\mu m s^{-1}$) as a function of force.

Chapter 4

Bidirectional Transport

Intracellular transport of a variety of cargo like organelles, nucleic acids, secretory vesicles, proteins, etc. is known to happen bi-directionally with the help of opposite-polarity molecular motors. This means that multiple motors take part in the transport of a single cargo, and instead of moving directly in one direction from the source to the sink, the molecular motors transport the cargo in a series of starts, reversal of directions and stops. The direction of the travel of cargo determines the dominating side of motors. Since the transport inside the cells is highly regulated, it seems that cells can control the 'net' transport of cargo. A few models have been proposed to explain the bi-directional motion of the cargo; namely 'Tug-of-War Model', 'Exclusionary Presence Model' and 'Co-ordination Model'. The tug-of-war model is one of the most popularly studied model among these.

4.1 Tug-of-War Model

As the name suggests, this model results in a tug-of-war like situation between the plus-end Kinesin motors and the minus-end Dynein motors. This means that the opposite polarity motors are attached to the cargo at the same time and both the sides of the motors try to pull away the cargo along with it. As a result of this, the instantaneously stronger side of motors take the cargo along with them. This unregulated stochastic pulling of cargo leads to frequent switching of the direction

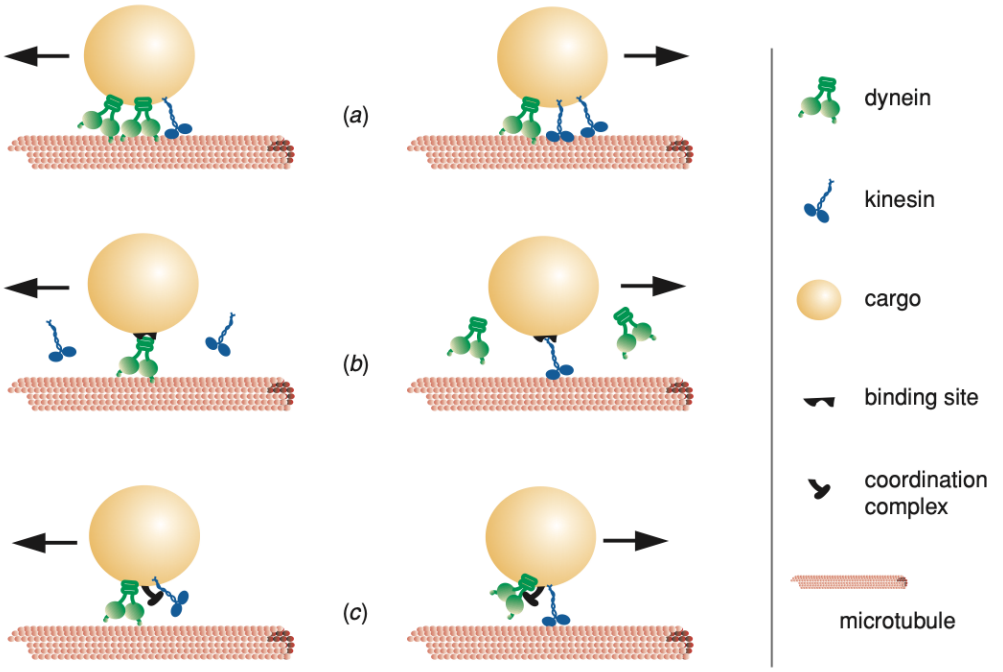

Figure 4.1: Different proposed models of intracellular bi-directional transport (Taken from [5]): (a) Tug-of-war Model; (b) Exclusionary Presence Model; (c) Co-ordination Model

of the transport of cargo. However, the 'net' transport direction within the cell is regulated by controlling the number of motors attached to the cargo. Hence, if a system follows this model, one would predict that in the absence of an opposing force for one direction (achieved by inhibiting the activity of the opposite side motors), there would be an enhancement of motility of cargo in that direction.

4.2 Paradox of co-dependence

According to the Tug-of-War model, if you switch off the activity of one type of motors, the cargo processivity increases in the other direction. However, it has been experimentally observed that turning off the activity of Kinesin motors did not lead to an enhancement of the cargo movement towards one end, which is opposite to what is expected from the tug-of-war model! This can imply that some sort of internal co-ordination mechanism exists, which results in an overall decline

in the motility of the cargo in one direction when the activity of the motors on the other side is inhibited [20]. This is counter-intuitive and the behaviour depicted by the system is referred to as the 'Paradox of Co-dependence'.

We put the catch bond behavior of dynein in the tug-of-war picture and try to see what happens from the brownian dynamics simulation. Within a mean field picture and stochastic Gillespie type simulations it has been predicted that using the catch bond can explain the above paradox [20]. However, in both these approaches it is assumed that the load is shared equally amongst the molecular motors. In our brownian dynamics simulations, we do not make such assumption. Some initial results of such simulation have been shown to agree with the predictions from mean field. Here, we do extensive simulations to see if the behavior across the parameter space can be observed.

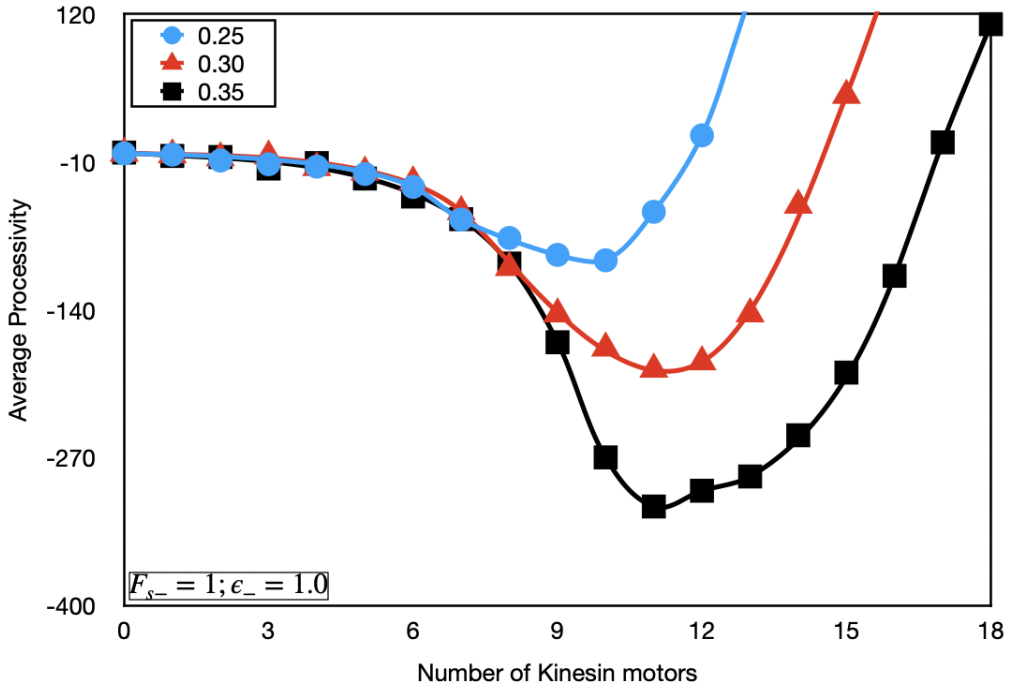

Figure 4.2: Average processivity as we change the number of kinesin motors for $F_{s-} = 1$ pN; $\epsilon_{0-} = 1.0/\text{sec}$; $N_{-} = 4$.

4.3 Results and Discussion

In this chapter, we look at the results obtained from the simulations carried out. All the systems are averaged over 100 trajectories. The system is allowed to run, at least, till $t = 10^4 sec$ or till all the motors get detached from the microtubule filament, whichever happens first.

4.4 The Average Cargo Processivity

The average cargo processivity is the average distance travelled by a cargo along the microtubule filament before all the motors get detached from the microtubule. We look at how the average processivity of the system evolves on changing various parameters of the system, like the number of motors, the dynein catch-bond strength, the size of the cargo bead etc, while keeping the other parameters constant.

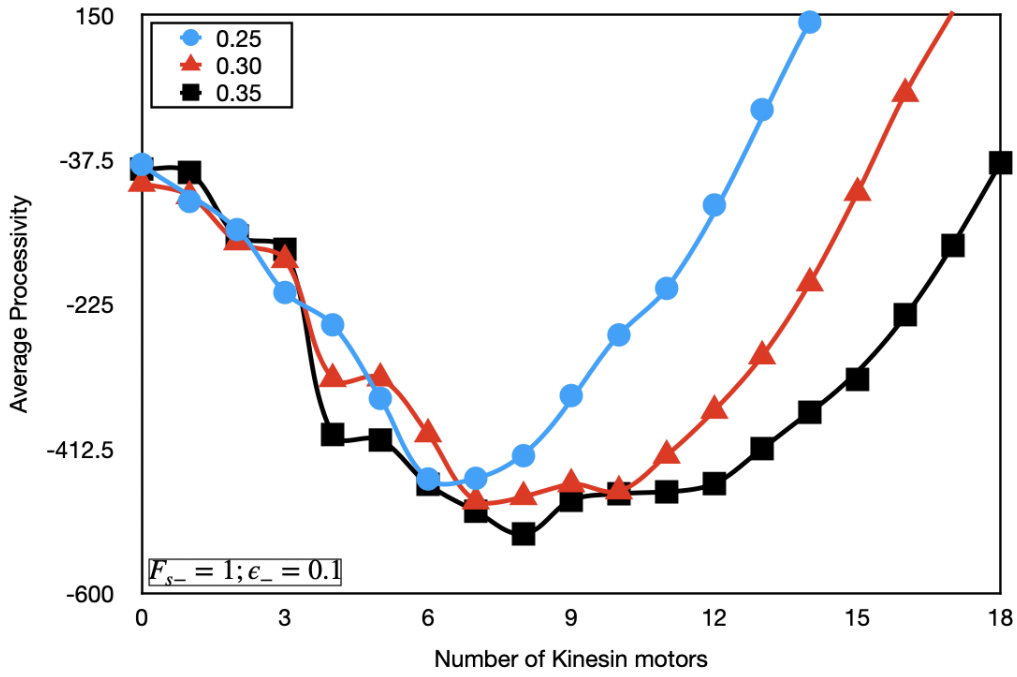

Figure 4.3: Cargo processivity as we change the number of kinesin motors for $F_{s-} = 1pN$; $\epsilon_{0-} = 0.1/\text{sec}$, $N_- = 4$.

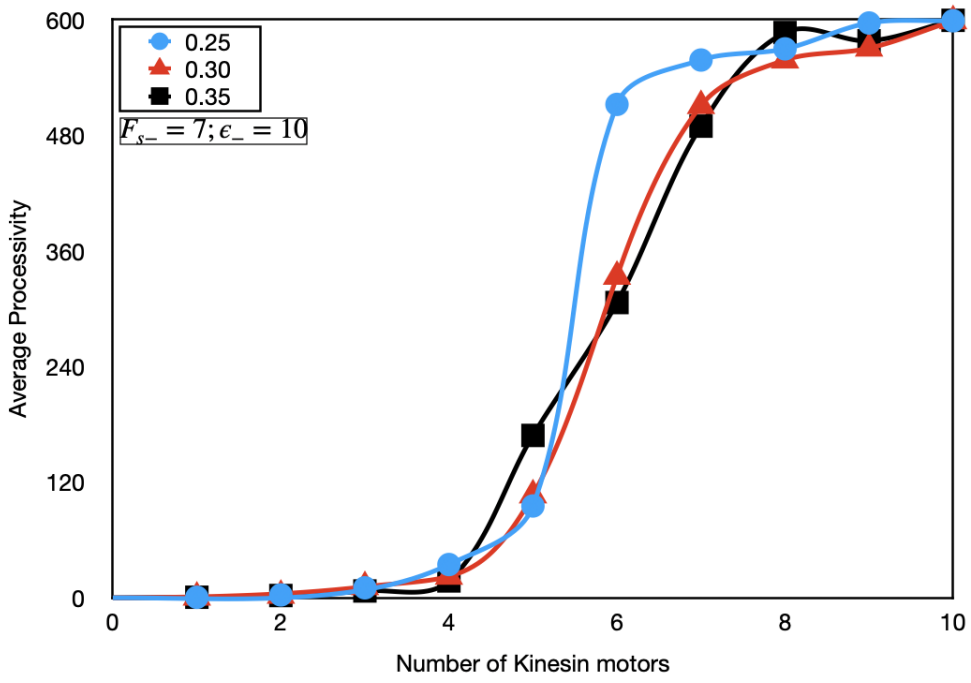

Figure 4.4: Average processivity as we change the number of kinesin motors for $F_{s-} = 7pN$; $\epsilon_{0-} = 10.0/\text{sec}$, $N_{-} = 4$.

4.4.1 Changing the number of molecular motors

Here, we change the number of one type of molecular motors, while keeping the number of other type of motors constant, to look at how the cargo processivity of the system varies. We also change the values of other parameters like the strength of the catch-bond, the size of the cargo bead, the dynein motor properties etc. to make a comparison.

In Fig. 4.2, we see that till $\sim$ 5 Kinesin motors, no significant motion in the cargo is observed. After that, we see a dip in average processivity indicating the activation of catch-bond regime. The system stays in the catch-bond regime as far as the number of kinesin motors do not overshoot and hence, start dominating. Also, the larger the cargo size, the greater is the amount of opposing force required to get the system out of the catch-bond regime.

In Fig. 4.3, we observe that the catch-bond gets activated even for lower number

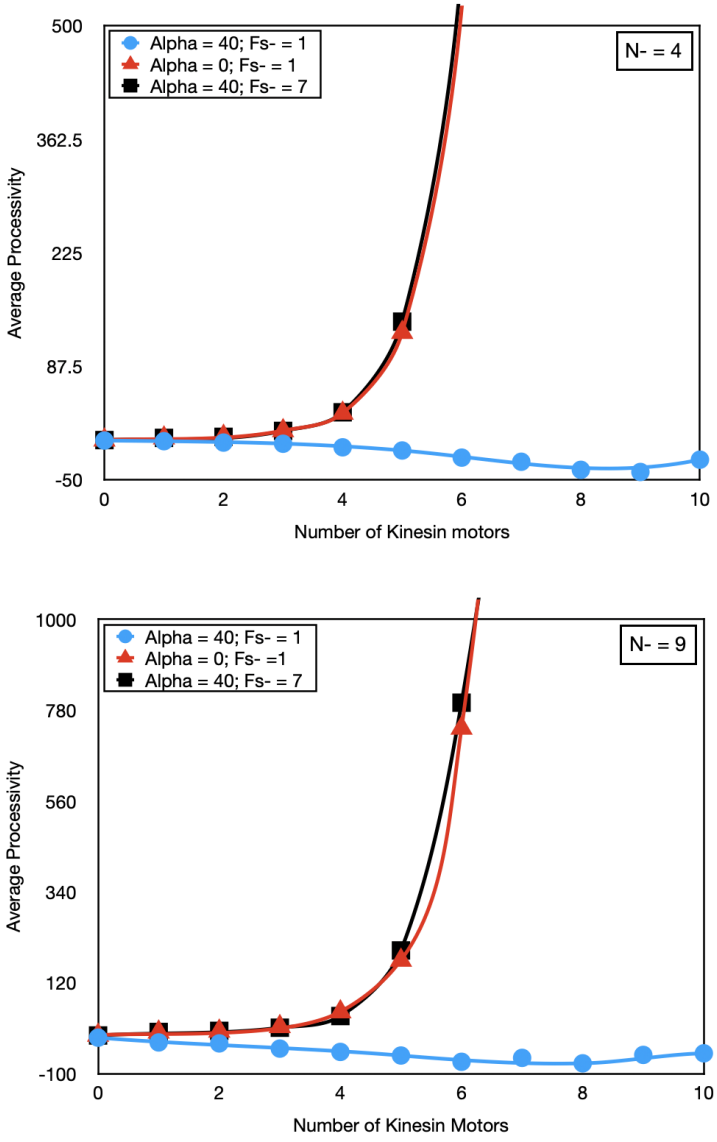

Figure 4.5: Average Processivity as a function of N_+, for (a.) $N_- = 4$; (b.) $N_- = 9$ for different dynein motor parameters.

of kinesin motors. This is achieved at lower bare unbinding rates. This indicates that the weaker the dynein motors, the faster the catch-bond regime gets activated. This can be supported by the fact that weaker dynein motors have lower stall force value and hence require lower opposing force for the catch-bond to get activated. As in the previous case, kinesin motors tend to dominate as their numbers increase.

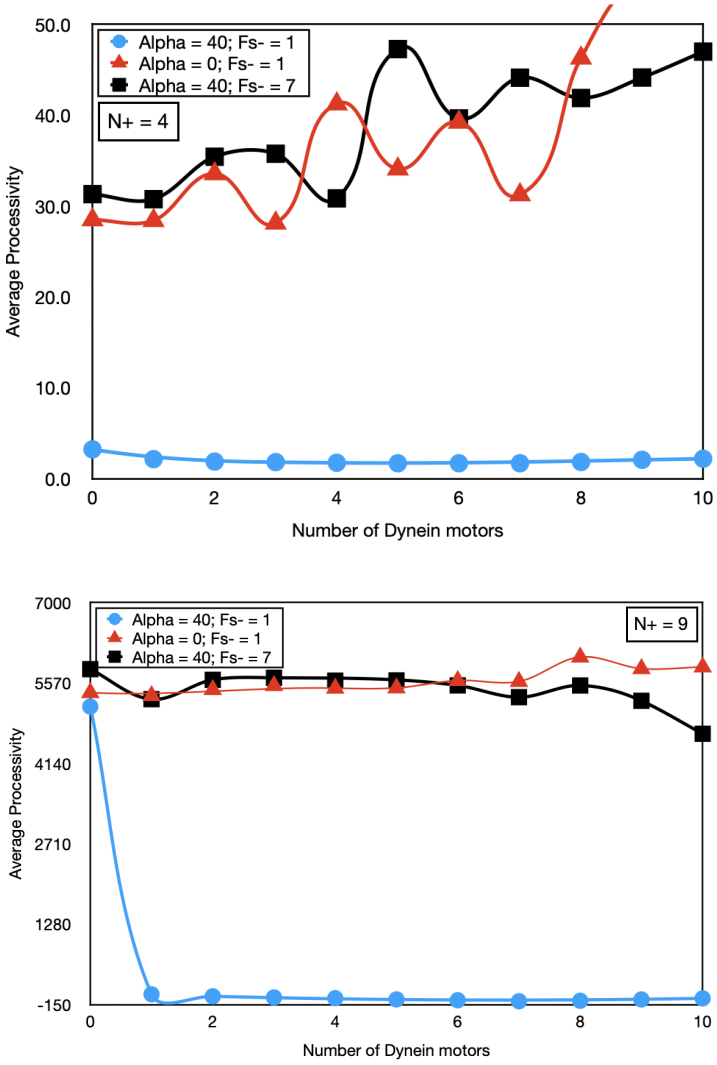

Figure 4.6: Average Processivity as a function of N_-, for (a.) $N_+ = 4$; (b.) $N_+ = 9$ for different dynein motor parameters.

Further, changing the size of the cargo has a similar effect to that observed for the higher unbinding rate.

In Fig. 4.4, the catch-bond never seems to get activated. This can be due to the higher value of the dynein stall force. So, a much greater opposing force is required to get the catch-bond regime activated. It seems that by the time

the desired opposing force value is reached, the number of kinesin motors start dominating. Here, the effect of cargo size is not prominent.

In Fig. 4.5 and Fig. 4.6, we see that for $F_{s-} = 1$ and $\alpha = 40$, the system behaves significantly different from the rest of the values of these variables. For low stall force of dynein, catch bond is turned on and we see a non-monotonic variation. For $F_{s-} = 7$, even when the catch bond is turned on, it is never really activated before getting unbound. The behavior therefore is close to what is observed for $\alpha = 0$ which essentially means that there is no catch-bond.

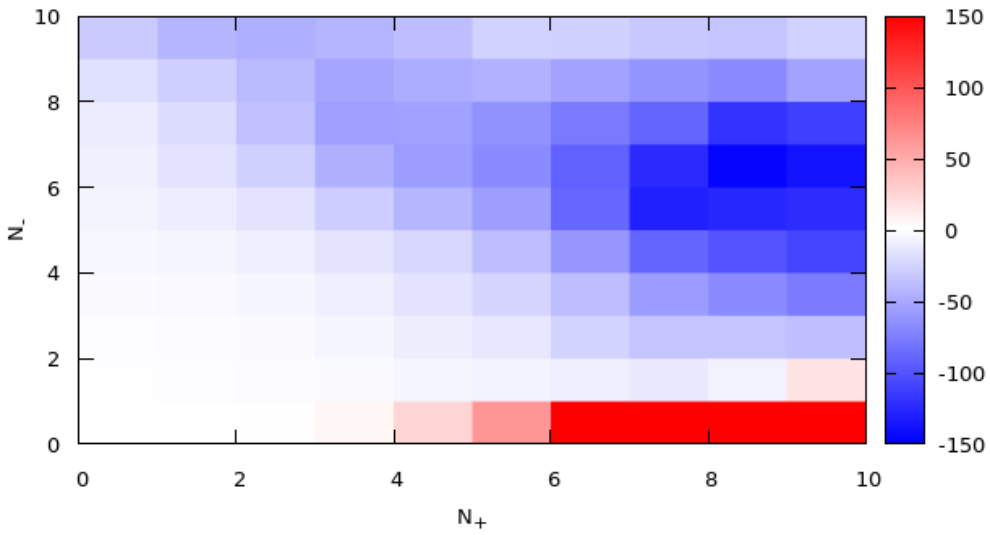

Figure 4.7: Phase diagram for average processivity in the $N_+ - N_-$ plane with $F_{s-} = 1pN$ and $\epsilon_{0-} = 1/sec$.

In Fig. 4.7 we construct the phase diagram for the average processivity in the $N_+ - N_-$ plane for low stall force of dynein where the catch-bond behavior is robust. As we can see from the contour plot, there is a distinct regime where the cargo predominantly moves in the negative direction although the number of kinesin motors are increased. This is the counter intuitive phenomenon that is paradox of codependence.

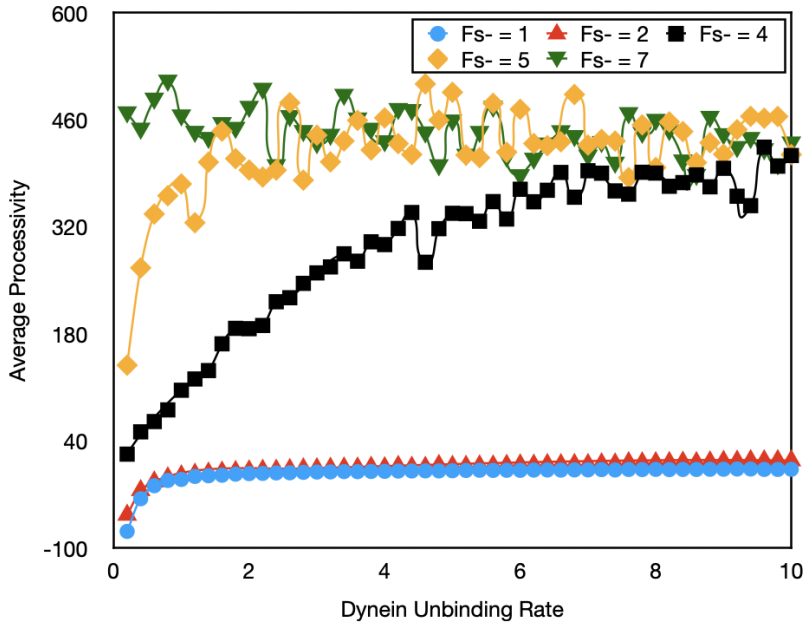

Figure 4.8: Average processivity for varying values of F_{s-} as a function of ϵ_{0-} ($N_+ = 6; N_- = 2$).

In Fig. 4.8, we plot the change of processivity as we changed the bare unbinding rate of dynein. Unbinding rates can be controlled in experiments. For low stall forces, the average processivity increases with ϵ_{0-} and saturates. With increasing stall forces, the saturation regime is changed. As the dynein stall force increases, the average processivity first increases rapidly and then, fluctuates around the same values ~ 500.

4.4.2 The strength of catch-bond

The strength of the Dynein catch-bond is one of the important factors in determining how the system evolves, especially the cargo processivity. In fig. 4.9, we look at the average processivity of a system with $N_+ = 6$ and $N_- = 2$ for three different values of α. For $\alpha = 20k_BT$, the average processivity of the system doesn't vary monotonically, as was expected. However, for $\alpha = 30k_BT$, the average processivity of the system remains nearly constant. For $\alpha = 40k_BT$, processivity decreases in the negative direction for lower values of ϵ_{0-} and eventually becomes constant.

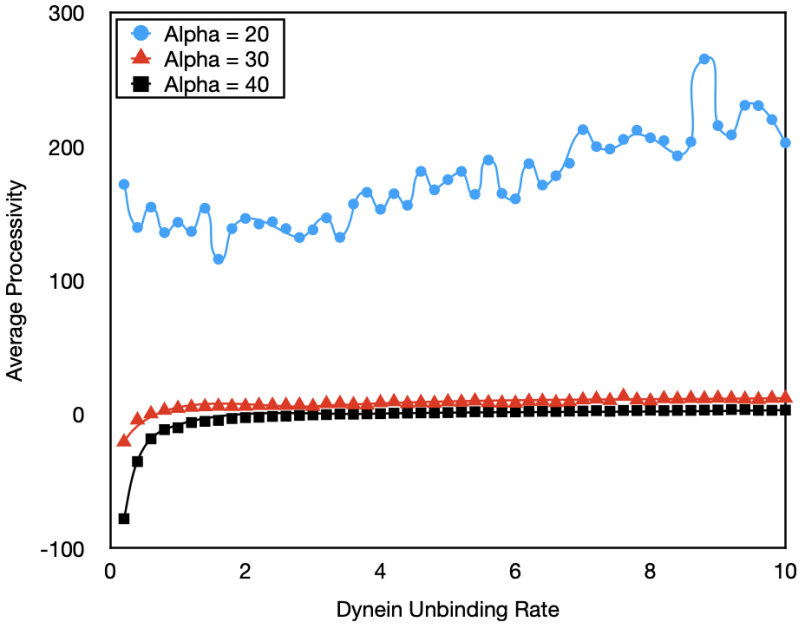

Figure 4.9: Average processivity as a function of ϵ_{0-} as we change the strength of Dynein catch-bond ($N_+ = 6; N_- = 2$).

4.5 Average no. of attached motors

We look at how the average number of kinesin and dynein motors attached to the microtubule change with changing number of total number of molecular motors available in the system. This helps in understanding the cargo processivity as processivity would hugely depend on the number of motors attached to the microtubule filament.

In Fig. 4.10 and Fig. 4.11, we observe the stark variations between the values of dynein properties when catch-bond is activated ($F_{s-} = 1; \alpha = 40$) versus when the catch-bond regime is not active. We see in Fig. 4.10a that in the absence of catch-bond, the average number of attached dynein motors decrease rapidly with increasing kinesin motors and in Fig. 4.11a, we see that the average number of attached kinesin motors increase almost linearly with increasing number of kinesin motors in the system. These observations suggest that the average processivity of these systems increase in the positive side when the catch-bond is inactive. However, when the catch-bond regime is active, a higher number of dynein motors

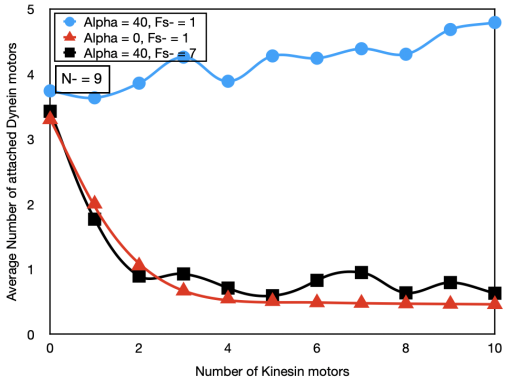

(a) $N_- = 9$

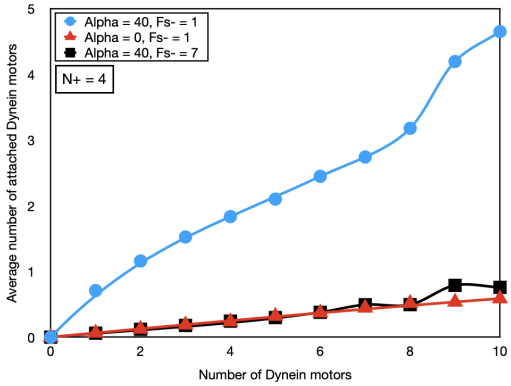

(b) $N_+ = 4$

Figure 4.10: Average number of bound Dyneins for varying number of motors in the system.

and a lesser number of kinesin motors remain attached on an average to the microtubule filament, leading to lower average cargo processivity as observed in Fig. 4.5.

In Fig. 4.10b, we observe that in the absence of catch-bond ($\alpha = 0$), the average number of attached dynein motors increase quite slowly with increasing Dynein motors. Similarly, for strong dynein motors ($F_{s-} = 7; \alpha = 40$), the average number of attached Dynein motors vary in a similar fashion. These observations suggest that the average processivity of these systems doesn't vary a lot when the catch-bond is inactive. However, when the catch-bond regime is active ($F_{s-} = 1pN; \alpha = 40k_BT$), the average number of attached dynein motors increase

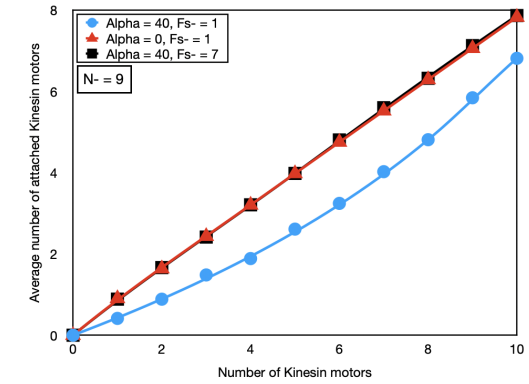

(a) $N_- = 9$

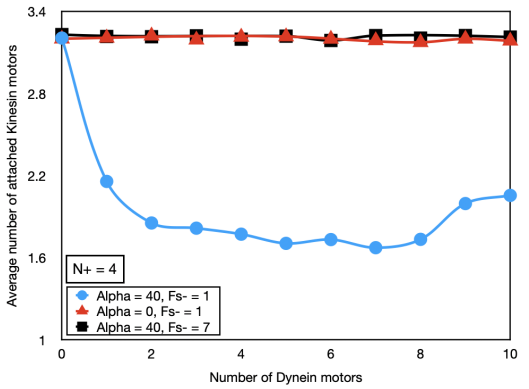

(b) $N_+ = 4$

Figure 4.11: Average number of bound Kinesins for varying number of motors in the system.

almost linearly with increasing number of dynein motors in the system and the number of attached kinesin motors that remain attached on an average to the microtubule filament decrease almost linearly for lower values of N_-. This value, then, starts increasing slowly as the number of dynein motors increase in the system. This means that the cargo activity would be towards the negative end as compared to when the catch-bond is not active, as observed in Fig. 4.6.

Chapter 5

Mean field theory

In this chapter, we discuss some analytical results that can be obtained within the mean field approximation that the load force is equally shared among all the bound motors. We look at a system with N_+ number of kinesin motors and N_- number of dynein motors, which move on a microtubule filament on one end and are attached to the cargo on the other side. These molecular motors attach and detach from the microtubule with attachment rates $\pi_\pm$ and detachment rates $\epsilon_\pm$. The state of the system, at a given point of time, is characterized by the number of attached motors, denoted by n_+ and n_- for kinesin and dynein motors respectively. At a given point of time, the probability of finding the system in a state with n_+ and n_- attached kinesin and dynein motors respectively can be denoted by $p\,(n_+, n_-)$. The Master Equation for such a system can be written as [20, 16]:

$$\begin{aligned}\frac{\partial p(n_+,n_-)}{\partial t} &= p(n_+ + 1, n_-)\epsilon_+(n_+ + 1, n_-) + p(n_+, n_- + 1)\epsilon_-(n_+, n_- + 1) \\ &+ p(n_+ - 1, n_-)\pi_+(n_+ - 1, n_-) + p(n_+, n_- - 1)\pi_-(n_+, n_- - 1) \\ &- p(n_+, n_-)\left[\epsilon_+(n_+, n_-) + \epsilon_-(n_+, n_-) + \pi_+(n_+, n_-) + \pi_-(n_+, n_-)\right]\end{aligned} \tag{5.1}$$

In such a system, the binding rates for Kinesin and Dynein motors are given as the following:

$$\pi_{\pm} = (N_{\pm} - n_{\pm})\,\pi_{0\pm} \tag{5.2}$$

Hence, for the first Kinesin and Dynein motors to be attached to the microtubule filament, the binding rate would be $N_{\pm}\pi_{0\pm}$.

The unbinding rates for these molecular motors depend on the force experienced by them as well as the type of bond they form with the microtubule filament. Since the Kinesin motors form slip-bond with the MT filament, the unbinding rate for these motors is given as:

$$\epsilon_{+}\,(n_{+}, n_{-}) = n_{+}\epsilon_{0+} exp\left(\frac{F_c\,(n_{+}, n_{-})}{n_{+}F_{d+}}\right) \tag{5.3}$$

The unbinding rate for Dynein motors is obtained from the Threshold Force Bond Deformation (TFBD) model as, where E_d is the deformation energy:

$$\epsilon_{-}\,(n_{+}, n_{-}) = n_{-}\epsilon_{0-} exp\left(-E_d\,(F_c) + \frac{F_c}{n_{-}F_{d-}}\right) \tag{5.4}$$

5.1 Incorporating the catch-bond

In the equation for unbinding rate for Dynein motors (3.4), the deformation energy term kicks in when the force experienced by the Dynein motor goes beyond the Dynein stall force, thereby entering the catch-bond regime. E_d is modelled by the following relation:

$$E_d\,(F_c) = \Theta\left(\frac{F_c}{n_{-}} - F_{s-}\right)\alpha\left[1 - exp\left(-\frac{\frac{F_c}{n_{-}} - F_{s-}}{F_0}\right)\right] \tag{5.5}$$

Here, the Θ function ensures that E_d comes into play only when $F_c > F_{S-}$, α determines the catch-bond strength and F_0 is the force scale for deformation energy.

In equations (3.3), (3.4) and (3.5), F_c is the co-operative force experienced by the motors as an effect from other motor species and $F_{d\pm}$ characterizes the detachment energy for the motor species.

Since the co-operative force has to depend on the number of motors attached

to the microtubule filament, it is expressed as:

$$F_c\left(n_+, n_-\right) = \frac{n_+ n_- F_{S+} F_{S-}}{n_- F_{S-} v_{0+} + n_+ F_{S+} v_{0-}} \left(v_{0+} + v_{0-}\right) \tag{5.6}$$

In the above equation, $F_{S\pm}$ denotes the stall forces and $v_{0\pm}$ represents the velocity of the respective molecular motors. The velocity of the cargo, which is expressed as:

$$v_c\left(n_+, n_-\right) = \frac{n_+ F_{S+} - n_- F_{S-}}{\frac{n_- F_{S-}}{v_{0-}} + \frac{n_+ F_{S+}}{v_{0+}}} \tag{5.7}$$

It is worth noting here that v_c is greater than 0 when the Kinesin motors exert more force on the cargo than the Dynein motors, which means $n_+ F_{S+} > n_- F_{S-}$. Similarly, v_c is lesser than 0 when $n_- F_{S-} > n_+ F_{S+}$ [12].

5.2 Mean First Passage Time

Mean First Passage Time (MFPT), denoted by $T(n_+, n_-)$, is the average time taken for a cargo to unbind from the microtubule filament to reach state $(0, 0)$, starting from (n_+, n_-) at time $t = 0$[12]. Since, in this system, we have two types of motors and the cargo would get attached to the microtubule filament, if either one of the motors gets attached to the filament. Hence, the effective unbinding rate is given by the following relation:

$$\epsilon_{eff} = \frac{1}{T(1,0) + T(0,1)} \tag{5.8}$$

Now, we define a recursive relation for $T(n_+, n_-)$, as given below [20]:

$$\begin{aligned} T(n_+, n_-) = \tau(n_+, n_-)[1 + \pi_+(n_+, n_-)T(n_+ + 1, n_-) + \pi_-(n_+, n_-)T(n_+, n_- + 1) \\ + \epsilon_+(n_+, n_-)T(n_+ - 1, n_-) + \epsilon_-(n_+, n_-)T(n_+, n_- - 1)] \end{aligned} \tag{5.9}$$

Here, $\tau(n_+, n_-)$ is the mean residence time defined as the time for which the system stays in a particular state [20]. It is expressed by:

$$\tau(n_+, n_-) = \frac{1}{\pi_+(n_+, n_-) + \pi_-(n_+, n_-) + \epsilon_+(n_+, n_-) + \epsilon_-(n_+, n_-)} \tag{5.10}$$

It is worth noting that eq. (5.9) is not applicable when the system is in (N_+, N_-) and $(0, 0)$ states. The boundary conditions for this system are as given below:

$$\begin{gathered} T(N_+, N_-) = \tau(N_+, N_-)[1 + \epsilon_+(N_+, N_-)T(N_+ - 1, N_-) + \epsilon_-(N_+, N_-)T(N_+, N_- - 1)] \\ T(0, 0) = 0 \end{gathered} \tag{5.11}$$

Here, $\tau(N_+, N_-)$ is given as $\tau_{N_+,N_-} = \frac{1}{\epsilon_+(N_+,N_-)+\epsilon_-(n_+,n_-)}$.

5.3 Cargo Processivity

As we defined a recursive relation for the first passage time, similarly, we can define a recursive relation for the average processivity of the cargo, $L(n_+, n_-)$. It is defined as the average distance the cargo travels before all the motors it is attached to, get detached from the microtubule. In a particular state (n_+, n_-), the distance travelled by the cargo is given by $\gamma(n_+, n_-) = v_c(n_+, n_-)\tau(n_+, n_-)$ [20]. Here, $v_c(n_+, n_-)$ is the velocity with which the cargo moves for (n_+, n_-) state and $\tau(n_+, n_-)$ is the mean residence time of the cargo in (n_+, n_-) state. So, we get the relation for average processivity for the cargo as:

$$\begin{aligned} L(n_+, n_-) = \gamma(n_+, n_-)[1 + \pi_+(n_+, n_-)L(n_+ + 1, n_-) + \pi_-(n_+, n_-)L(n_+, n_- + 1) \\ + \epsilon_+(n_+, n_-)L(n_+ - 1, n_-) + \pi_-(n_+, n_-)L(n_+, n_- - 1)] \end{aligned} \tag{5.12}$$

As earlier, here we have $L(0, 0) = 0$. We average over a large number of trajectories, so we have

$$\langle L(n_+, n_-)\rangle_{n_+n_-} = K\Sigma_{n_+=0}^{N_+}\Sigma_{n_-=0}^{N_-}L(n_+, n_-)\left[1 - \delta_{n_++n_-,0}\right] \tag{5.13}$$

We have K as a normalization factor here, which is given as $K = \frac{1}{(N_+ + 1)(N_- + 1) - 1}$ [20].

Bibliography

[1] Barsegov, V., and Thirumalai, D. Probing protein-protein interactions by dynamic force correlation spectroscopy. *Physical Review Letters 95*, 16 (Oct. 2005).

[2] Bartolo, D., Derényi, I., and Ajdari, A. Dynamic response of adhesion complexes: Beyond the single-path picture. *Physical Review E 65*, 5 (May 2002).

[3] Cortes, D., Gordon, M., Nédélec, F., and Maddox, A. Bond type and discretization of non-muscle myosin ii are critical for simulated contractile dynamics. *bioRxiv* (2019).

[4] Evans, E., Leung, A., Heinrich, V., and Zhu, C. Mechanical switching and coupling between two dissociation pathways in a p-selectin adhesion bond. *Proceedings of the National Academy of Sciences 101*, 31 (July 2004), 11281–11286.

[5] Gross, S. P. Hither and yon: a review of bi-directional microtubule-based transport. *Physical Biology 1*, 2 (jun 2004), R1–R11.

[6] Herrmann, H., Bär, H., Kreplak, L., Strelkov, S. V., and Aebi, U. Intermediate filaments: from cell architecture to nanomechanics. *Nature Reviews Molecular Cell Biology 8*, 7 (2007), 562–573.

[7] Hirokawa, N., Niwa, S., and Tanaka, Y. Molecular motors in neurons: Transport mechanisms and roles in brain function, development, and disease. *Neuron 68*, 4 (2010), 610 – 638.

[8] hong Xia, C., Rahman, A., Yang, Z., and Goldstein, L. S. Chromosomal localization reveals three kinesin heavy chain genes in mouse. *Genomics 52*, 2 (1998), 209 – 213.

[9] Jolly, A. L., and Gelfand, V. I. Bidirectional intracellular transport: utility and mechanism. *Biochemical Society transactions 39*, 5 (10 2011), 1126–1130.

[10] Kardon, J. R., and Vale, R. D. Regulators of the cytoplasmic dynein motor. *Nature Reviews Molecular Cell Biology 10*, 12 (2009), 854–865.

[11] Karki, S., and Holzbaur, E. L. Cytoplasmic dynein and dynactin in cell division and intracellular transport. *Current Opinion in Cell Biology 11*, 1 (1999), 45 – 53.

[12] Klumpp, S., and Lipowsky, R. Cooperative cargo transport by several molecular motors. *Proceedings of the National Academy of Sciences 102*, 48 (2005), 17284–17289.

[13] Kunwar, A., Tripathy, S. K., Xu, J., Mattson, M. K., Anand, P., Sigua, R., Vershinin, M., McKenney, R. J., Clare, C. Y., Mogilner, A., et al. Mechanical stochastic tug-of-war models cannot explain bidirectional lipid-droplet transport. *Proceedings of the National Academy of Sciences 108*, 47 (2011), 18960–18965.

[14] Mallik, R., Carter, B. C., Lex, S. A., King, S. J., and Gross, S. P. Cytoplasmic dynein functions as a gear in response to load. *Nature 427*, 6975 (2004), 649.

[15] Mallik, R., Rai, A. K., Barak, P., Rai, A., and Kunwar, A. Teamwork in microtubule motors. *Trends in cell biology 23*, 11 (2013), 575–582.

[16] Müller, M. J. I., Klumpp, S., and Lipowsky, R. Motility states of molecular motors engaged in a stochastic tug-of-war. *Journal of Statistical Physics 133*, 6 (2008), 1059.

[17] Nair, A., Chandel, S., Mitra, M. K., Muhuri, S., and Chaudhuri, A. Effect of catch bonding on transport of cellular cargo by dynein motors. *Physical Review E 94*, 3 (2016), 032403.

[18] Novikova, E. A., and Storm, C. Contractile fibers and catch-bond clusters: a biological force sensor? *Biophysical Journal 105*, 6 (Sept. 2013), 1336–1345.

[19] Pereverzev, Y. V., and Prezhdo, O. V. Dissociation of biological catch-bond by periodic perturbation. *Biophysical Journal 91*, 2 (July 2006), L19–L21.

[20] Puri, P., Gupta, N., Chandel, S., Naskar, S., Nair, A., Chaudhuri, A., Mitra, M. K., and Muhuri, S. Dynein catch bond as a mediator of codependent bidirectional cellular transport. *Phys. Rev. Research 1* (Sep 2019), 023019.

[21] Ross, J. L., Ali, M. Y., and Warshaw, D. M. Cargo transport: molecular motors navigate a complex cytoskeleton. *Current opinion in cell biology 20*, 1 (02 2008), 41–47.

[22] Schliwa, M. *Molecular Motors*. Springer Berlin Heidelberg, Berlin, Heidelberg, 2006.

[23] Schroer, T. A. Dynactin. *Annual Review of Cell and Developmental Biology 20*, 1 (2004), 759–779. PMID: 15473859.

[24] Welte, M. A. Bidirectional transport along microtubules. *Current Biology 14*, 13 (2004), R525 – R537.

[25] Woehlke, G., and Schliwa, M. Directional motility of kinesin motor proteins. *Biochimica et Biophysica Acta (BBA) - Molecular Cell Research 1496*, 1 (2000), 117 – 127.